

Short communication

# Novel Al<sub>2</sub>O<sub>3</sub>-based compressive seals for IT-SOFC applications

Shaobai Sang, Wei Li, Jian Pu, Li Jian\*

*College of Material Science and Engineering, Huazhong University of Science and Technology, State Key Laboratory of Material Processing and Die & Mould Technology, 1037 Luo Yu Road, Hubei, Wuhan 430074, PR China*

Received 9 August 2007; received in revised form 26 October 2007; accepted 31 October 2007

Available online 6 November 2007

## Abstract

Novel compressive Al<sub>2</sub>O<sub>3</sub>-based seals were developed and characterized under simulated intermediate temperature solid oxide fuel cell (IT-SOFC) environment. The seals were prepared by tape casting, mainly composed of fine Al<sub>2</sub>O<sub>3</sub> powder with various contents of fine Al powder addition. The leakage rates were determined at 800 °C under 0.14–0.69 MPa compressive stresses, and the stabilities were evaluated at 750 °C under constant 0.35 MPa compressive stress. The leakage rates at 800 °C were in range of 0.2–0.01 sccm cm<sup>-1</sup>, decreasing with increasing the compressive stress and Al content; Al addition significantly improved the stability, the leakage rate with 20 wt% Al addition was as low as 0.025 sccm cm<sup>-1</sup> at 800 °C under 0.35 MPa compressive stress with a gauge pressure of 6.9 kPa, and exhibited good stability at 750 °C. Single cell test also confirmed the effectiveness of the tape cast Al<sub>2</sub>O<sub>3</sub>-based seal for planar IT-SOFC applications.

© 2007 Elsevier B.V. All rights reserved.

*Keywords:* SOFC; Compressive seal; Al<sub>2</sub>O<sub>3</sub>; Al; Leak rate

## 1. Introduction

Featured by reduced operation temperature, high power density, simple configuration, easy assembly, metallic interconnects and low cost manufacturing, the planar IT-SOFCs have attracted intensive attention since the end of last century [1]; however, one of the most significant challenges in the planar design is to develop effective high temperature seals to prevent fuel/oxidant gas leakage and provide electrical insulation within the stack [2,3]. The seal needs to have sufficient structural/chemical stabilities itself and thermal/chemical compatibilities with adjacent cell and interconnect components under the SOFC operating conditions.

So far, majority of SOFC seals development have been focused on rigid glass or ceramic-glass materials [2], deformable metallic materials [4,5] and mica-base seals [3,6–10]. The advantage of glass based seals is that their compositions can be tailored to optimize the required physical properties, such as the coefficient of thermal expansion (CTE); nevertheless, they tend to change in phases and react with the cell component materials and interconnects under SOFC operating conditions in a

long run, because of the intrinsic thermodynamical instability [11,12]. The plain mica is virtually incompressible; a considerable compressive stress is required to obtain satisfied sealing effect, which may cause cell breakages. The hybrid mica-based seals [7–9] have achieved quite low leakage rate, but the sealing processes become more complex and other issues, such as stability and compatibility, have remained unsolved. The application of the deformable metallic seals is limited by its high electronic conductivity. In general, more robust sealing materials are desired to overcome the sealing difficulty in the planar SOFC design.

In the paper, novel Al<sub>2</sub>O<sub>3</sub>-based compressive seals and associated fabrication technique were reported. The seals were mainly composed of fine Al<sub>2</sub>O<sub>3</sub> powder with fine Al powder addition, and prepared by tape casting. The effectiveness of the seals was confirmed by simulated out-of-cell and cell tests; and discussed in terms of the microstructural characterizations.

## 2. Experimental

### 2.1. Seal preparation

The characteristics and providers of the starting materials used in this investigation were summarized in Table 1. Fig. 1

\* Corresponding author. Tel.: +86 27 87557694; fax: +86 27 87557694.  
E-mail address: [plumarow@126.com](mailto:plumarow@126.com) (L. Jian).

Table 1  
The used raw materials and providers

Component	Material	Provider
Powder	Al <sub>2</sub> O <sub>3</sub> , $d_{10} = 1.2 \mu\text{m}$ , $d_{50} = 3.5 \mu\text{m}$ , $d_{90} = 7.1 \mu\text{m}$ Al, $d_{10} = 0.7 \mu\text{m}$ , $d_{50} = 1.5 \mu\text{m}$ , $d_{90} = 2.4 \mu\text{m}$	Kunming Institute of Precious Metals Beijing Mountain Technical Development Center for Non-ferrous Metals
Solvent	Ethanol/dimethylbenzene, volume ratio: 1:2	Tianjin No.3 Chemical Reagent Factory
Dispersant	Menhaden fish oil	Richard E. Mistler Inc.
Binder	Polyvinyl butyral-76 (PVB-76)	Solutia Inc.
Plasticizer	Butyl benzyl phthalate (BBP) Polyalkylene glycol (PAG)	Wuhan Organic Synthesis Factory Richard E. Mistler Inc.

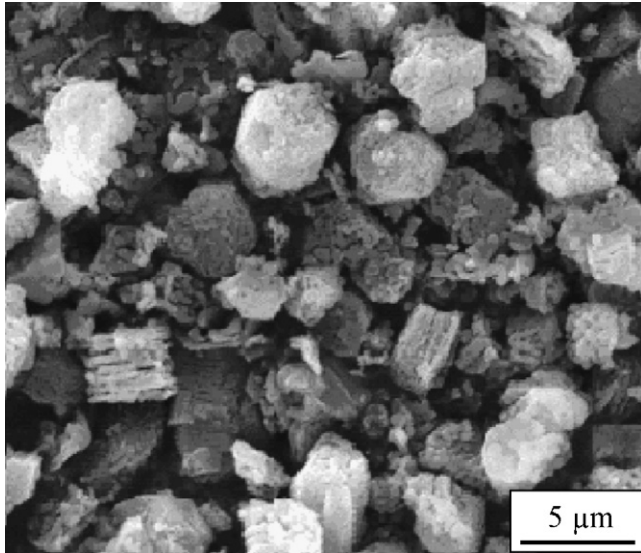


Fig. 1. SEM photograph of the used Al<sub>2</sub>O<sub>3</sub> powders.

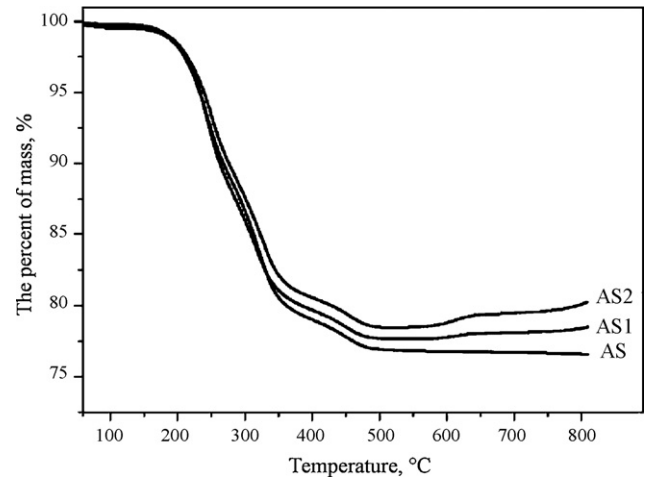


Fig. 2. Thermogravimetric graph of the tape cast AS, AS1 and AS2 samples.

is the scanning electron microscope (SEM, QUANTA 200, FEI) photograph of the raw Al<sub>2</sub>O<sub>3</sub> powders. The compressive Al<sub>2</sub>O<sub>3</sub>-based seals were prepared by tape casting, and the organic additives and their quantities used in the tape casting process are shown in Table 2. The thickness of the compressive seals is around 0.38 mm, and no defects were observed on the surfaces. One important characteristic of the compressive seals is that they have good flexibility at room temperature, and can be pressed on the sealing surfaces easily under moderate compressive stresses. Fig. 2 is the thermogravimetric curves of the cast tapes in air for the designated AS, AS1 and AS2 samples, respectively, obtained by using a DT-A7 thermal analysis system of Perkin-Elmer Inc. with a heating rate of 10 °C min<sup>-1</sup>, which was used to guide the temperature profile during heating for the sealing tests.

Table 2  
Tape casting formulations for the Al<sub>2</sub>O<sub>3</sub>-based seals

Sample	Al <sub>2</sub> O <sub>3</sub> powder	Al powder	Solvent	Fish oil	P PVB-76	BBP	PAG
AS	100		42	2	8.5	8	8.5
AS1	90	10	42	2	8.5	8	8.5
AS2	80	20	42	2	8.5	8	8.5

## 2.2. Out-of-cell leak test and post-test characterization

The leak test samples were prepared as a window frame with an outside dimension of 7 cm by 7 cm and an inside dimension of 5 cm by 5 cm, as shown in Fig. 3. The leak tests were conducted by an in-house designed set-up, schematically shown in Fig. 4. The window frame specimen was placed in between two polished stainless steel plates under a compressive load. The volume of gas reservoir was 200 cm<sup>3</sup>, and the pressure in the gas reservoir was adjusted and stabilized at 3.5, 6.9 and 10.3 kPa, respectively. The flow reading from the rotometer (FL-310, OMGEA engineering Inc., USA) represented the leakage of the seals, once the equilibrium of the flow was reached. The leak rate was determined by the flow reading divided by the inside perimeter of the window frame samples.

According to the thermogravimetric analysis of the cast tapes, the samples were heated in a half furnace at a heating rate of 2 °C min<sup>-1</sup> to 200 °C, and dwelled at 200 °C for 90 min followed by further heating at 3 °C min<sup>-1</sup> up to 750 °C or 800 °C. The

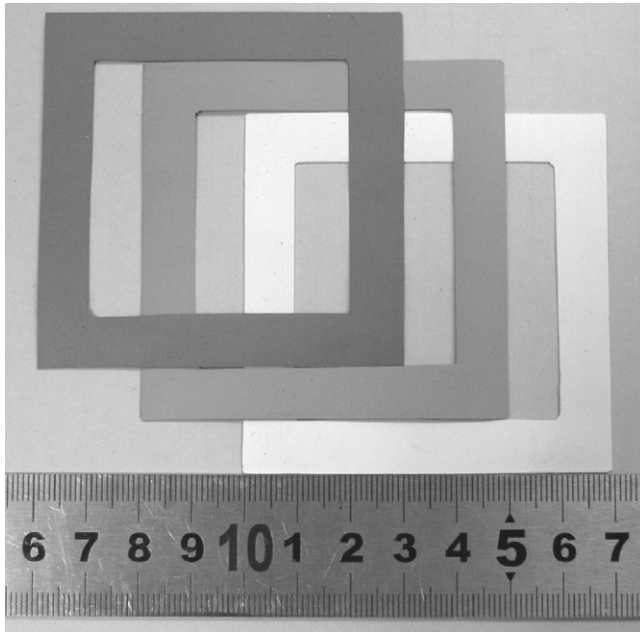


Fig. 3. Photograph of samples for the leak test.

leakage was measured under various compressive stresses from 0.14 to 0.69 MPa at 800 °C, and the durability was evaluated under a constant compressive stress of 0.35 MPa at 750 °C. The leak rate of a phlogopite paper sample with the same dimension was measured under the same circumstances for comparison. The microstructures of the fracture surfaces of the post-test samples were examined by SEM (QUANTA 200, FEI) for explanation of the test results.

### 2.3. Cell test

In order to assess the sealing capability in applications, a single cell test with the developed seal was carried out. The anode supported planar SOFC cell of an active area of 9 cm × 9 cm with conventional cell component materials was prepared by tape casting/screen printing/co-firing processes. The test jig was made of SS430 steel plates with gas channels. The square window frame seals, with an outside dimension of 10 cm by 10 cm and an inside dimension of 9 cm by 9 cm, were placed between the cell and the testing jig plates under a compressive load of

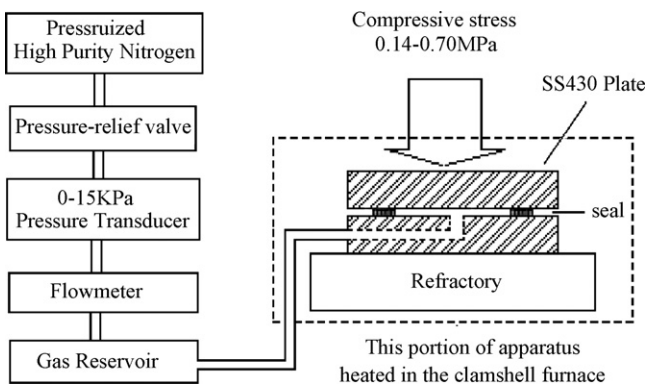


Fig. 4. Schematic set-up of the compressive seal test.

0.2 MPa. Pure H<sub>2</sub> was used as the fuel and air as the oxidant, and the test was conducted at 750 °C. The open circuit voltage (OCV) was measured at 750 °C; durability test at a current density of 494 mA cm<sup>-2</sup> was conducted for 5000 s.

## 3. Results and discussion

### 3.1. Leakage of compressive Al<sub>2</sub>O<sub>3</sub>-based seals

Table 3 shows the leak rate of the developed Al<sub>2</sub>O<sub>3</sub>-based compressive seals and phlogopite paper at 800 °C under 0.14–0.69 MPa, with gauge pressures of 3.5 kPa (a), 6.9 kPa (b), 10.3 kPa (c), respectively. Obviously, the leak rate of all samples decreased with increasing of the compressive stress; however, the leakage rate of the Al<sub>2</sub>O<sub>3</sub>-based seals, in the range of 0.2–0.01 sccm cm<sup>-1</sup>, is much lower than that of the phlogopite paper. With increasing Al addition from 0 to 20 wt%, the leak rate under 0.69 MPa compressive stress and 6.9 kPa gauge pressure significantly decreased from 0.044 to 0.009 sccm cm<sup>-1</sup>. For the AS2 sample, the leak rate approached zero under the same compressive stress with a smaller gauge pressure of 3.5 kPa, although insignificant fluctuation was observed. Generally, the leak rates obtained in the present study are much lower than those of the single layer compressive seals, such as phlogopite paper [3,7,13], muscovite paper and single crystal [3,7]; similar to those of the silica infiltrated fiber paper [13], phlogopite paper + glass and muscovite paper + glass [7]; and slightly higher than those of the hybrid mica-based seals such as muscovite SC + glass [7], muscovite SC + Ag [8], H<sub>3</sub>BO<sub>3</sub> infiltrated phlogopite + glass and infiltrated phlogopite + glass [9].

Table 3

The leak rate (sccm cm<sup>-1</sup>) of the Al<sub>2</sub>O<sub>3</sub>-based seals and phlogopite paper at 800 °C under compressive stresses 0.14–0.69 MPa, and gauge pressures 3.5 kPa (a), 6.9 kPa (b) and 10.3 kPa (c)

Seal	Compressive stress (MPa)	Gauge pressure		
		3.5 kPa	6.9 kPa	10.3 kPa
AS	0.14	0.133	0.228	0.349
	0.21	0.080	0.122	0.196
	0.35	0.051	0.096	0.158
	0.48	0.037	0.067	0.101
	0.69	0.020	0.044	0.067
AS1	0.14	0.045	0.115	0.175
	0.21	0.031	0.090	0.133
	0.35	0.015	0.047	0.069
	0.48	0.010	0.038	0.049
	0.69	0.007	0.013	0.028
AS2	0.14	0.030	0.062	0.119
	0.21	0.021	0.048	0.085
	0.35	0.009	0.025	0.042
	0.48	0.007	0.014	0.031
	0.69	~0	0.009	0.017
Phlogopite paper	0.14	0.875	1.332	1.791
	0.21	0.771	1.187	1.625
	0.35	0.708	1.042	1.292
	0.48	0.625	0.917	1.125
	0.69	0.542	0.792	0.958

In previous studies [9,13,14], it was identified that there are two possible paths for mica-base seal leak: one is through mica itself; the other is through the interfaces between mica and the adjacent SOFC components. The interfaces are considered as the major leak paths of conventional mica seals. Higher compressive stresses ensure a closer contact between the phlogopite paper and the SS430 plate, reducing the leakage through the interfaces, and in the mean time, make the phlogopite paper denser, shutting down some of the leak paths in side the mica. As a consequence, the overall leak rate is decreased as the compressive stress is increased. Similar explanation can be applied to the effect of compressive stress on the leak rate for the tape cast  $\text{Al}_2\text{O}_3$ -based seals. The difference is that the tape cast  $\text{Al}_2\text{O}_3$ -based seals have excellent flexibility and deformability at room temperature, which redounds a tight contact between the seal and the SS430 plates, resulting in a much lower leakage rate than that of the phlogopite paper seal. This consideration is supported by the low room temperature leakage of  $0\text{--}0.02\text{ sccm cm}^{-1}$  for the tape cast  $\text{Al}_2\text{O}_3$ -based seals. Even though the organic additives in the tape cast  $\text{Al}_2\text{O}_3$ -based seals are burnt out, the remaining fine  $\text{Al}_2\text{O}_3$  particles still tightly match with the SS430 plate under compressive stress. The squiggly leak paths in the fine porous  $\text{Al}_2\text{O}_3$  body, instead of the direct leak paths between the flakes in the sandwich layer-structured phlogopite paper [6] will generate tremendous leak resistance, which is the another reason for the low leak rate of the tape cast  $\text{Al}_2\text{O}_3$ -based seals contrasted to the phlogopite paper seals.

Comparing the  $\text{Al}_2\text{O}_3$ -based seals with different Al contents, it was found that the leak rate decreased remarkably with increasing the content of Al powder with the same testing condition. For example, the leak rate of the AS2 sample (20 wt% Al addition) at  $800\text{ }^\circ\text{C}$  is  $0.025\text{ sccm cm}^{-1}$  under a gauge pressure  $6.9\text{ kPa}$  and a compressive stress  $0.35\text{ MPa}$ , which is around a half of the leak rate ( $0.047\text{ sccm cm}^{-1}$ ) for the AS1 sample (10 wt% Al addition) and a quarter of that ( $0.096\text{ sccm cm}^{-1}$ ) for the AS sample (0 wt% Al addition).

Fig. 5 shows the microstructure of the fractured surfaces for the AS, AS1 and AS2 samples that were tested under a  $0.21\text{ MPa}$  compressive stress, respectively. It is obvious that the microstructure becomes denser with the addition of Al powder. The microstructure of the AS sample is somewhat loose;  $\text{Al}_2\text{O}_3$  particles are piled together, presenting a porous structure with basically submicron pores. Bigger pores in the neighborhood of a few microns are also observed in between particle clusters or agglomerates. The testing temperature is relatively low compared to the sintering temperature, no meaningful sintering occurred during the test. As well known, the leak resistance of the porous body is related to its porosity and pore size distribution. When the pore size is reduced to submicron scale, the leak resistance will dramatically increase. That is why a low leak rate was obtained with the  $\text{Al}_2\text{O}_3$ -based seals, even without Al addition. In the cases with Al addition, two possibilities that will further increase the density of the porous body, in turn, decrease the leak rate may happen. First, the Al particles become soft or liquid during heating and are squeezed into the surrounding pores, especially the bigger pores; second, oxidation of Al to  $\text{Al}_2\text{O}_3$  will give rise to a volume expansion of 28%, which will lower the

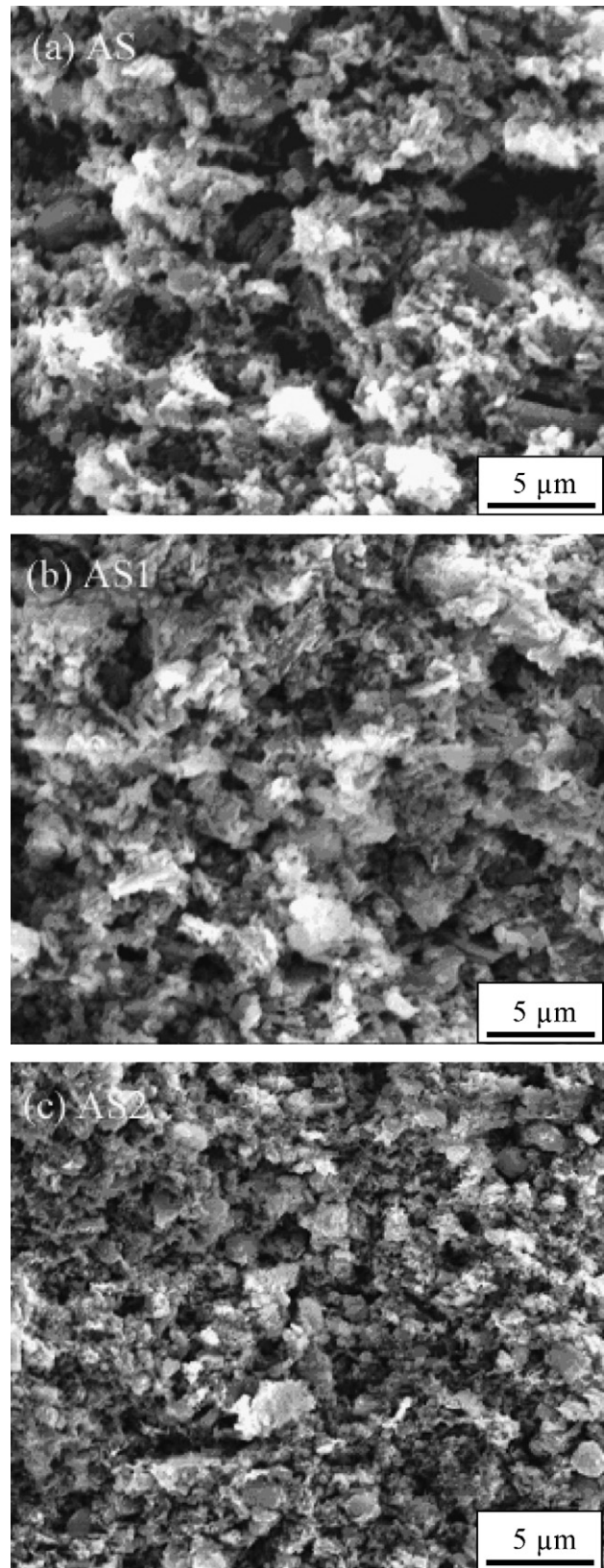


Fig. 5. SEM microstructures of the fractured surfaces for the post-test AS (a), AS1 (b) and AS2 (c) samples.

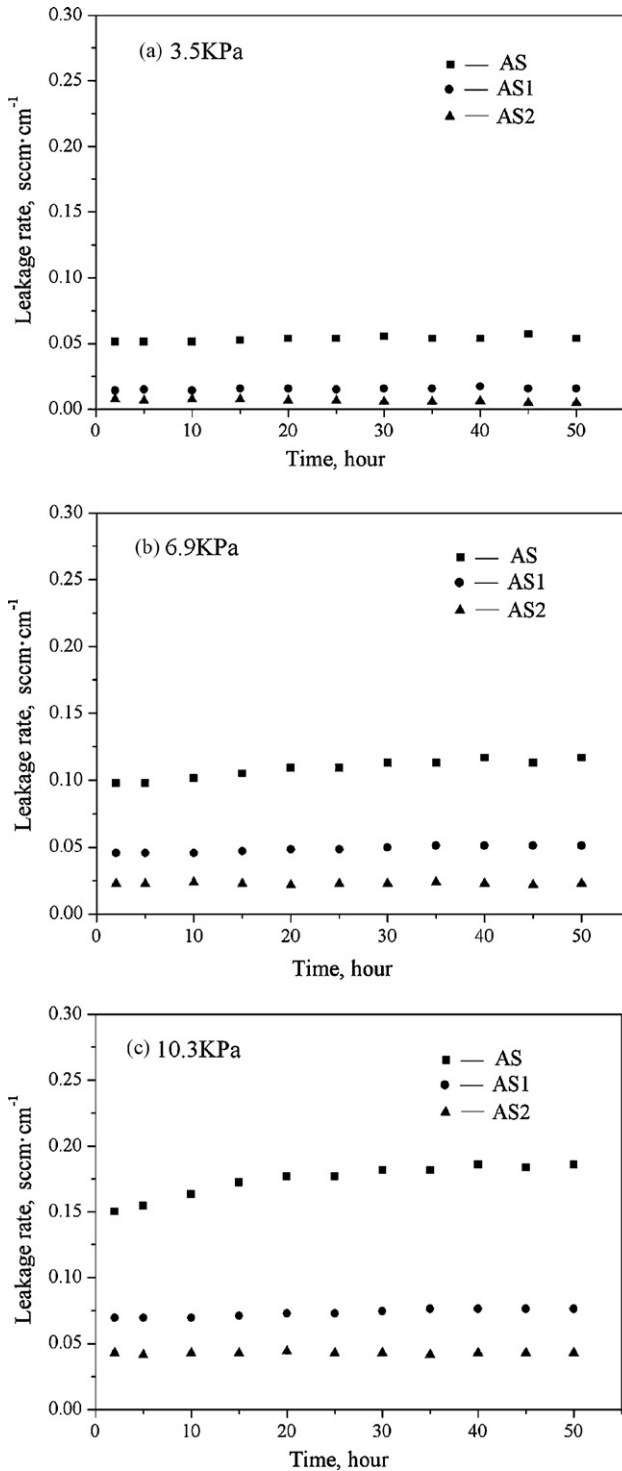


Fig. 6. Stability of the tape cast Al<sub>2</sub>O<sub>3</sub>-based seals at 750 °C, compressive stress 0.35 MPa and gauge pressure 3.5 kPa (a), 6.9 kPa (b), 10.3 kPa (c), respectively.

porosity accordingly when the seal is under compression stress and no overall volume change is allowed. From Fig. 5(b) and (c), it can be seen that the bigger pores in between the Al particle clusters become less and less observed, most of the big leak paths are closed. On the other hand, when Al particles are oxidized to form Al<sub>2</sub>O<sub>3</sub>, a reaction bond may be generated between the Al<sub>2</sub>O<sub>3</sub> particles, bringing them closer and increasing the tortu-

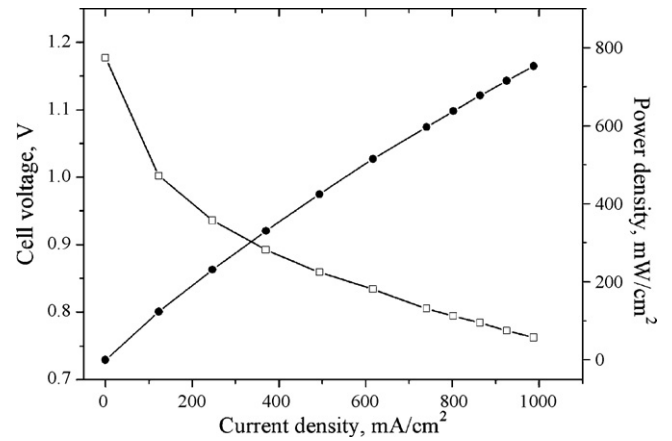


Fig. 7. Power curve of single cell test with the AS2 seal at 750 °C.

osity the leak paths and the leak resistance, and in the mean time, the seal will become stronger than that without Al addition. The above considerations are confirmed by the denser microstructures and much reduced leak rates of the Al-added tape cast Al<sub>2</sub>O<sub>3</sub> seals, as demonstrated by the microstructures in Fig. 5 and the leak rate data in Table 3.

### 3.2. Stability of compressive Al<sub>2</sub>O<sub>3</sub>-based seals

The stability of the tape cast Al<sub>2</sub>O<sub>3</sub> based seals was evaluated at 750 °C under 0.35 MPa compressive stress with various gauge pressure according to the requirement of the planar IT-SOFC application. Fig. 6 shows the stability results for the AS, AS1 and AS2 samples at gauge pressure 3.5 kPa (a), 6.9 kPa (b) and 10.3 kPa (c), respectively. The stability of the AS sample is not as satisfied as the Al-added seals, and becomes worse with gauge pressure increase. Tested for 50 h, the leak rate of the AS sample was enhanced by 12% from 0.051 to 0.057 sccm cm<sup>-1</sup> at 3.5 kPa gauge pressure; by 19% from 0.098 to 0.117 sccm cm<sup>-1</sup> at 6.9 kPa gauge pressure; and by 23% from 0.151 to 0.186 sccm cm<sup>-1</sup> at 10.3 kPa gauge pressure. In contrast, the leak rate of the AS1 and the AS2 samples

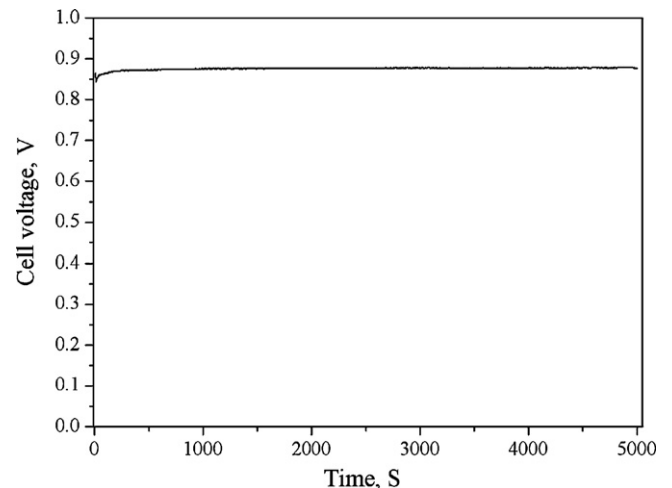


Fig. 8. Single cell performance with the AS2 seal.

remained stable during 50 h of test, only small fluctuation was observed.

The stability difference is attributed to the microstructures of the seals. The microstructures of the fractured surfaces of the  $\text{Al}_2\text{O}_3$ -based seals were examined after the stability test. Microstructures similar to Fig. 4 were observed. It is expected that the less bonded loose microstructure of the AS sample be not strong enough to survive higher gauge pressure, new leak paths may be formed in the weakly linked area. The higher the gauge pressure, the greater the possibility is to generate new leak paths. The denser and reaction bonded microstructures of the AS1 and the AS2 samples are able to maintain stability during the test under the designated gauge pressures, resulting in an almost unchanged leak rate.

### 3.3. Applicability of compressive $\text{Al}_2\text{O}_3$ -based seals

Based on the leak rate and stability results, the AS2 sample was selected for 10 cm by 10 cm planar SOFC cell test. Fig. 7 is the power curve; a high open circuit voltage of 1.17 was achieved, which is close to the theoretic value. Fig. 8 is the performance curve of the single cell, the voltage maintained stable at 877 mV under a current density of  $494 \text{ mA cm}^{-2}$  during the testing time. This single cell test demonstrated the applicability of the tape cast  $\text{Al}_2\text{O}_3$ -based seals in planar IT-SOFCs.

## 4. Conclusion

$\text{Al}_2\text{O}_3$ -based compressive seals with Al addition of 0, 10, and 20 wt% were fabricated by tape cast technique. Simulated out-of-cell leak test and single cell test were conducted. The post-test microstructures of the seals were characterized. The following conclusions can be made.

- (1) The  $\text{Al}_2\text{O}_3$ -based tape cast seals have much better sealing effect than that of the mica seals, such as phlogopite paper.
- (2) With Al addition from 0 to 20 wt%, the post-test microstructure becomes denser, big pores in between  $\text{Al}_2\text{O}_3$  particle

clusters are sealed by Al. The leak rate decreases with Al content increase.

- (3) Al-added tape cast  $\text{Al}_2\text{O}_3$ -based seals have long-term stable performance, which is attributed to the denser microstructure and stronger connection between particles caused by the formed reaction bonds while Al is converted to  $\text{Al}_2\text{O}_3$ .
- (4) The developed Al-added tape cast  $\text{Al}_2\text{O}_3$ -based seals is proved to be applicable in planar IT-SOFCs by the single cell test.

## Acknowledgements

This project is financially supported by National “863” program of China under the contract 2006AA05Z148, Wuhan Science and Technology Bureau key project 200710321087 and Asia Zirconium Limited. SEM analysis was assisted by the Analytical and Testing Center of Huazhong University of Science and Technology.

## References

- [1] S.C. Singhal, J. Mizusaki (Eds.), Solid oxide fuel cells-IX, the Electrochemical Society Proceedings, Pennington, NJ, 2005.
- [2] W.F. Jeffrey, J. Power Sources 147 (2005) 46–57.
- [3] S.P. Simner, J.W. Stevenson, J. Power Sources 102 (1/2) (2001) 310–316.
- [4] K.S. Weil, J.S. Hardy, Ceram. Eng. Sci. Proc. 25 (3) (2004) 321–326.
- [5] J. Duquette, A. Petric, J. Power Sources 137 (1) (2004) 71–75.
- [6] Y.S. Chou, J.W. Stevenson, J. Power Sources 124 (2) (2003) 473–478.
- [7] Y.S. Chou, J.W. Stevenson, L.A. Chick, J. Power Sources 112 (1) (2002) 130–136.
- [8] Y.S. Chou, J.W. Stevenson, L.A. Chick, J. Am. Ceram. Soc. 86 (6) (2003) 1003–1007.
- [9] Y.S. Chou, J.W. Stevenson, J. Power Sources 135 (1/2) (2004) 72–78.
- [10] Y.S. Chou, J.W. Stevenson, P. Singh, Ceram. Eng. Sci. Proc. 26 (4) (2004) 257–264.
- [11] S.P. Jiang, L. Christiansen, B. Hughan, K. Fogger, J. Mater. Sci. Lett. 20 (8) (2001) 695–697.
- [12] Z. Yang, J.W. Stevenson, K.D. Meinhardt, Solid State Ionics 160 (2003) 213–225.
- [13] S. Le, K. Sun, N. Zhang, J. Power Sources 161 (2006) 901–906.
- [14] Y.S. Chou, J.W. Stevenson, P. Singh, J. Power Sources 152 (2005) 168–174.